Experimental Evaluation of Passive 2D Optical Beam Scanners for FMCW LiDAR Applications

Mennatallah Kandil[(1),(2)], Mathias Prost[(1)], Ana Lebanov[(1)], Jon Ø. Kjellman[(1)], Wim Bogaerts[(2)], Marcus S. Dahlem[(1)]

[(1)] IMEC, Kapeldreef 75, 3001 Leuven, Belgium, menna.kandil@imec.be, marcus.dahlem@imec.be
[(2)] Ghent University - IMEC, Photonics Research Group, Gent, Belgium, wim.bogaerts@ugent.be

Abstract *We present the first experimental demonstration of a pixelated dispersive optical phased array (DOPA). For the same aperture design, the fabricated pixelated DOPA shows improved side lobe suppression ratio compared to the continuous DOPA by up to* −6 dB *around* 1550 nm. *©2024 The Author(s)*

Introduction

The realization of a solid-state light detection and ranging (LiDAR) engine that fulfills the requirements of the automotive industry is an ongoing research challenge[1]. The main functionalities of a LiDAR engine are beam steering and ranging. The former sends a narrow beam in a certain farfield direction, while the latter detects the back-scattered signal and measures the distance to the target. Optical phased arrays (OPAs) are a potential implementation of the beam scanning functionality[2].

Two-dimensional beam scanning using on-chip OPAs can be achieved with active tuning of a 2D array of antennas with phase shifters in the light distribution network[2]. While conceptually simple, this approach is challenging in terms of circuit density, power consumption and control complexity. Alternatively, one can steer a beam in two dimensions using an OPA through the manipulation of a single variable: the wavelength of a tunable laser. In such OPAs, a 1D array of long waveguide grating-based antennas is used together with cumulative delay lines in the optical distribution network. The light is steered in one direction (the *slow axis*) due to the wavelength-dependent emission angle of the waveguide gratings (the antennas), while in the other direction (the *fast axis*) the beam is steered due to the optical path length difference between the antennas[3]. This implementation, which we call a *continuous dispersive optical phased array* (DOPA), results in continuous scan lines in the 2D farfield when sweeping the laser wavelength.

However, continuous DOPAs have limited scalability due to compounding phase errors, propagation losses, and footprint of the distribution network[4]. For example, the effect of phase errors is observed in the literature of continuous DOPAs in the form of degraded sidelobe suppression ratio (SLSR)[5],[6]. Therefore, the *pixelated DOPA* concept was proposed[4] to reduce the total length of the delay lines across the distribution network by decoupling the specification on beam divergence and the farfield sampling resolution.

In this paper, we experimentally demonstrate the pixelated DOPA concept with an unbalanced splitter tree architecture. First, we characterize the performance of a continuous DOPA with a similar distribution tree network, after which we compare its performance with the pixelated device.

Device working principle and design

A DOPA steers the light along the slow axis according to the diffraction grating acting as an antenna, where the emission angle is a function of wavelength.

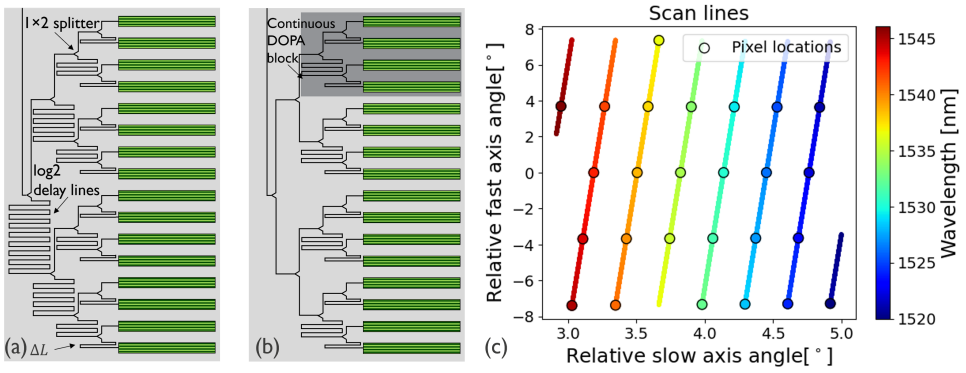

Fig. 1: DOPA variations: (a) schematic of the 16-element continuous DOPA implemented with an unbalanced splitter tree network; (b) schematic of the 16-element pixelated DOPA, where the distribution network is subdivided into four 4-element continuous DOPA blocks; (c) calculation of the farfield scan lines of the continuous DOPA, and pixel locations of the pixelated DOPA.

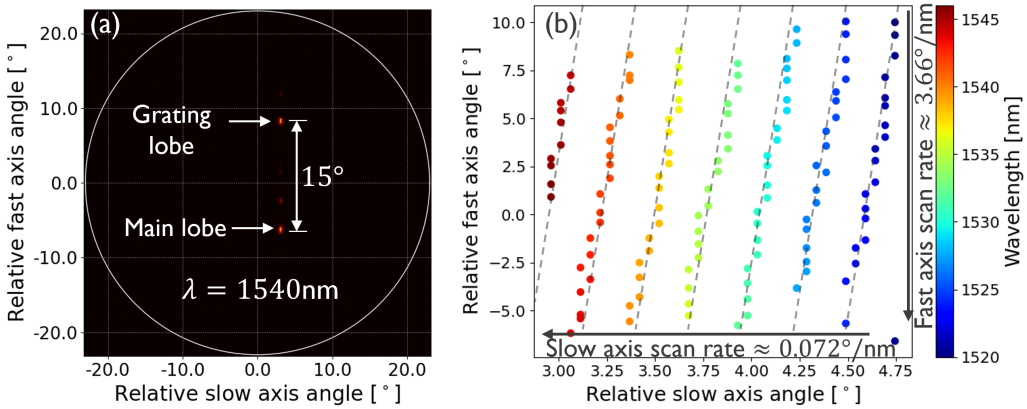

Fig. 2: Measurement of the continuous DOPA: (a) farfield at 1540 nm, showing grating lobe separation of ≈15°; (b) beam steering for wavelengths from 1520 nm to 1546 nm with a 0.02 nm step, showing scan rates of 3.66 °/nm for the fast axis and 0.072 °/nm for the slow axis, respectively.

To steer the beam along the fast axis, the grating antennas are arranged in a 1D array, and fed by waveguide delay lines with a constant length increment ΔL, as shown in Fig. 1(a). The phase difference $\Delta\phi$ between two adjacent antennas is a function of the wavelength λ, due to the optical path length difference:

$$\Delta\phi = 2\pi \frac{\Delta L . n_{eff}(\lambda)}{\lambda}, \tag{1}$$

where n_{eff} is the effective refractive index of the delay line. As the delay ΔL is typically much longer than the periodicity of the antenna grating, the scanning rate is much faster, hence the name *fast axis*. Increasing ΔL means that $\Delta\phi$ will sweep faster through the $[0, 2\pi]$ interval, leading to denser scan lines in the farfield. Thus, the specification of the number of scan lines determines the design choice of the delay line length:

$$\Delta L = \frac{\lambda^2_{center}}{n_g} . \frac{N_{lines}}{\Delta\lambda}, \tag{2}$$

where $\Delta\lambda$ and λ_{center} are the span and the center of the laser tuning range, respectively. n_g is the group index of the delay line and N_{lines} is the desired number of scan lines. The motion of the beam within the scan lines is illustrated in Fig. 1(c).

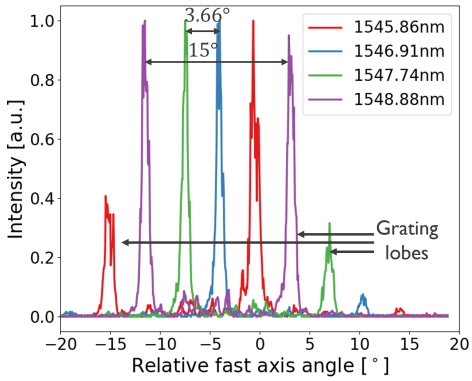

Fig. 3: Beam steering measurement of the pixelated DOPA, showing 4 consecutive pixels separated by ≈3.66° and ≈1 nm in wavelength.

Equations 1 and 2 apply to both the continuous and pixelated DOPAs. For the pixelated DOPA, shown in Fig. 1(b), the antenna array is the same as the continuous DOPA, but the distribution network is subdivided into smaller blocks. This means that the light emitted by the antennas will interfere constructively only at specific wavelengths, resulting in a discrete set of points on a scan line with a collimated spot, as shown in Fig. 1(c), hence, the name *pixelated*.

Fabrication

We fabricated a small-scale continuous and pixelated DOPAs with the same emitting aperture design, consisting of 16 grating-based antennas spaced 6 µm apart, corresponding to a separation between the main lobe and the grating lobe of 15° along the fast axis. Their distribution networks are based on an unbalanced splitter tree, as illustrated in Figs. 1(a),(b). The two devices are fabricated in an LPCVD SiN stack in imec's 200 mm pilot-line. This platform has low propagation losses and low phase errors compared to silicon platforms[7]. The shortest delay line length ΔL is 300 µm, and is calculated based on equation 2 to yield 25 scan lines over a 100 nm wavelength tuning range.

The distribution network of the pixelated DOPA is subdivided into four blocks which are fed by a balanced splitter tree, as shown in Fig. 1(b). The longest delay line length is reduced from 9.6 mm in the continuous DOPA device to 1.2 mm in the pixelated DOPA device. Reducing the length of the delay lines also reduces the overall insertion loss and phase errors, such that the pixelated DOPA is expected to outperform the continuous DOPA on side lobe suppression ratio.

Experimental results and discussion

The fabricated devices are characterized using a Fourier imaging setup. As shown in Fig. 2(a) and Fig. 3, the grating lobe separation of both devices is measured to be ≈15°, in agreement with theory. The beam is steered with a rate of 3.66 °/nm in

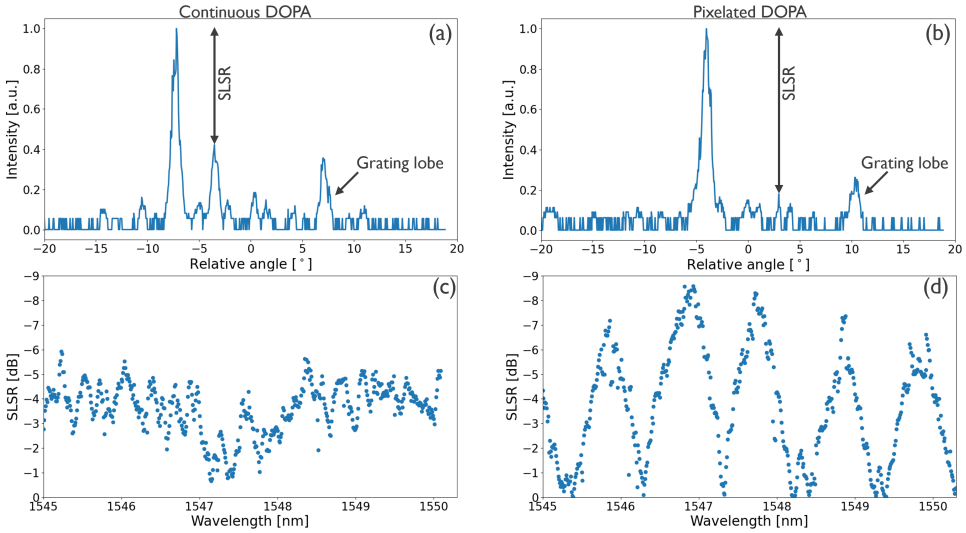

Fig. 4: Measurements results of the SLSR of the fabricated devices: (a,b) SLSR at λ =1546.91 nm for the continuous and pixelated DOPAs, respectively; (c,d) SLSR at wavelengths from 1545 nm to 1550 nm.

the fast axis and 0.072 °/nm in the slow axis, as shown in Fig. 2(b) and Fig. 3.

The pixelated DOPA beam steering is shown in Fig. 3, where the constructive interference wavelengths are separated by ≈1 nm leading to farfield sampling of ≈3.66°. This leads to ≈4 pixels per scan line, depending on the exact wavelength range of the scan line.

In order to evaluate whether there is an improvement in the beam quality of the pixelated DOPA compared to the continuous DOPA, we measure the SLSR of the two devices at different wavelengths. In order to extract the SLSR, we followed a method similar to Hutchison *et al.*[8] to compensate for any non-linearity of the camera.

Theoretically, OPAs with uniform power over the aperture input have sidelobe suppression ratio of ≈–13.26 dB at emission angle of 0°[9]. However, state-of-the-art DOPAs exhibit SLSRs of –3 dB to –10 dB[5],[6], where the values vary based on the fabrication technology, the distribution network architecture choice and the device scale, i.e. the number of antennas and the smallest delay length. This is due to variations in the effective refractive index of the waveguide caused by fabrication variations. These variations lead to deviations in the optical path lengths in the distribution network, which in turn causes errors on the input phase of the antennas. These phase errors will distort the wavefront and degrade the beam quality.

In our continuous DOPA, the emitted beam exhibits an SLSR with a mean value of –3.6 dB. As an example, the SLSR at λ =1549.91 nm is shown in Fig. 4(a). The best measured values over λ = 1500 nm-1600 nm are around –8 dB (not shown in the figure), which is comparable to other DOPAs in the literature. The variation of the SLSR with wavelength (farfield angle), shown in Fig. 4(c), is also in accordance with literature of OPAs[10],[11].

For the pixelated DOPA, the SLSR is higher than the continuous DOPA by ≈–2 dB to –6 dB, but only around the *operation* wavelengths where we have a collimated beam *pixel*, as shown in Figs. 4(b),(d). This suggests that the pixelated DOPA can still operate in a range around these pixels: the reduced length of waveguide delays helps it maintain a higher SLSR than the continuous one for a significant bandwidth around the operation wavelengths.

This available bandwidth is specifically important for swept source FMCW LiDAR, where the beam steering and ranging are done with the same wavelength variable[12]. To perform the FMCW ranging, the tunable laser needs to sweep over a bandwidth of a few GHz, while maintaining its focus on the same pixel with a good SLSR. In this comparison, the pixelated DOPA maintains a higher SLSR than the continuous DOPA for 30 % to 40 % of the wavelength spacing between the pixels. In this small-scale demonstration, this separation amounts to 50 GHz. In a scaled-up version, the number of pixels per scan line (corresponding with the number of delay line blocks) and the number of scan lines would increase, corresponding to a useful pixel bandwidth of 1 GHz to 3 GHz.

Conclusions

We experimentally compared the continuous and pixelated flavours of the dispersive OPA, demonstrating 2D beam scanning with a field of view of 15°. The devices exhibit a high SLSR compared to other reported DOPAs, up to ≈–10 dB. We showed a considerable improvement in the SLSR for the pixelated DOPA in a wide bandwidth around its operation wavelengths, as opposed to the corresponding continuous DOPA, which has a lower, but more uniform SLSR.

References

[1] R. Roriz, J. Cabral, and T. Gomes, "Automotive LiDAR Technology: A Survey", *IEEE Transactions on Intelligent Transportation Systems*, vol. 23, no. 7, pp. 6282–6297, 2022. DOI: 10.1109/TITS.2021.3086804.

[2] M. J. Heck, "Highly integrated optical phased arrays: photonic integrated circuits for optical beam shaping and beam steering", *Nanophotonics*, vol. 6, no. 1, pp. 93–107, 2017. DOI: doi:10.1515/nanoph-2015-0152.

[3] K. Van Acoleyen, W. Bogaerts, and R. Baets, "Two-Dimensional Dispersive Off-Chip Beam Scanner Fabricated on Silicon-On-Insulator", *IEEE Photonics Technology Letters*, vol. 23, no. 17, pp. 1270–1272, 2011. DOI: 10.1109/LPT.2011.2159785.

[4] W. Bogaerts, S. Dwivedi, R. Jansen, X. Rottenberg, and M. S. Dahlem, "A 2D Pixelated Optical Beam Scanner Controlled by the Laser Wavelength", *IEEE Journal of Selected Topics in Quantum Electronics*, vol. 27, no. 1, pp. 1–12, 2021. DOI: 10.1109/JSTQE.2020.3017230.

[5] N. Dostart, B. Zhang, A. Khilo, *et al.*, "Serpentine optical phased arrays for scalable integrated photonic lidar beam steering", *Optica*, vol. 7, no. 6, pp. 726–733, Jun. 2020. DOI: 10.1364/OPTICA.389006.

[6] P. Muñoz, D. Pastor, L. A. Bru, *et al.*, "Scalable Switched Slab Coupler Based Optical Phased Array on Silicon Nitride", *IEEE Journal of Selected Topics in Quantum Electronics*, vol. 28, no. 5: Lidars and Photonic Radars, pp. 1–16, 2022. DOI: 10.1109/JSTQE.2022.3162577.

[7] A. Rahim, J. Goyvaerts, B. Szelag, *et al.*, "Open-Access Silicon Photonics Platforms in Europe", *IEEE Journal of Selected Topics in Quantum Electronics*, vol. 25, no. 5, pp. 1–18, 2019. DOI: 10.1109/JSTQE.2019.2915949.

[8] D. N. Hutchison, J. Sun, J. K. Doylend, *et al.*, "High-resolution aliasing-free optical beam steering", *Optica*, vol. 3, no. 8, pp. 887–890, Aug. 2016. DOI: 10.1364/OPTICA.3.000887.

[9] C. A. Balanis, *Antenna theory: analysis and design*. John wiley & sons, 2016, ISBN: 9781119178989.

[10] T. Komljenovic, R. Helkey, L. Coldren, and J. E. Bowers, "Sparse aperiodic arrays for optical beam forming and LiDAR", *Optics Express*, vol. 25, no. 3, pp. 2511–2528, Feb. 2017. DOI: 10.1364/OE.25.002511.

[11] Y. Wang, G. Zhou, X. Zhang, *et al.*, "2D broadband beamsteering with large-scale MEMS optical phased array", *Optica*, vol. 6, no. 5, pp. 557–562, May 2019. DOI: 10.1364/OPTICA.6.000557.

[12] W. Bogaerts, M. Kandil, and M. S. Dahlem, "Integrated Optical Beam Scanning and FMCW Ranging using Multiplexed Tunable Lasers", in *2022 IEEE Photonics Conference (IPC)*, 2022, pp. 1–2. DOI: 10.1109/IPC53466.2022.9975452.